



Pre-stimulus alpha activity modulates long-lasting unconscious feature integration

Maëlan Q. Menétrey^{*}, Michael H. Herzog, David Pascucci

Laboratory of Psychophysics, Brain Mind Institute, École Polytechnique Fédérale de Lausanne (EPFL), Lausanne, Switzerland

ARTICLE INFO

Keywords:

Alpha oscillations
Pre-stimulus effects
Long-lasting feature integration
Unconscious processing

ABSTRACT

Pre-stimulus alpha (α) activity can influence perception of shortly presented, low-contrast stimuli. The underlying mechanisms are often thought to affect perception exactly at the time of presentation. In addition, it is suggested that α cycles determine temporal windows of integration. However, in everyday situations, stimuli are usually presented for periods longer than ~ 100 ms and perception is often an integration of information across space and time. Moving objects are just one example. Hence, the question is whether α activity plays a role also in temporal integration, especially when stimuli are integrated over several α cycles. Using electroencephalography (EEG), we investigated the relationship between pre-stimulus brain activity and long-lasting integration in the sequential metacontrast paradigm (SQM), where two opposite vernier offsets, embedded in a stream of lines, are unconsciously integrated into a single percept. We show that increases in α power, even 300 ms before the stimulus, affected the probability of reporting the first offset, shown at the very beginning of the SQM. This effect was mediated by the systematic slowing of the α rhythm that followed the peak in α power. No phase effects were found. Together, our results demonstrate a cascade of neural changes, following spontaneous bursts of α activity and extending beyond a single moment, which influences the sensory representation of visual features for hundreds of milliseconds. Crucially, as feature integration in the SQM occurs before a conscious percept is elicited, this also provides evidence that α activity is linked to mechanisms regulating unconscious processing.

1. Introduction

For almost a century, the relationship between perception and brain rhythms has been a central topic of research (Bishop, 1932; Adrian and Matthews, 1934; Latour, 1967). Many studies have focused on the role of alpha rhythm (α ; 8–13 Hz) (for review, see VanRullen and Dubois, 2011; Galloto et al., 2017; Van Diepen et al., 2019; Kienitz et al., 2022; Quigley, 2022) showing, for instance, that low pre-stimulus α power can improve visual detection and discrimination performance (Ergenoglu et al., 2004; Hanslmayr et al., 2005; van Dijk et al., 2008), and different phases of the α cycle can affect the rate of hits and misses in detection tasks (Busch et al., 2009; Mathewson et al., 2009). The interpretation of these findings often relies on the idea that α rhythm reflects alternating states of cortical inhibition and excitation, with higher α power at specific phases leading to more inhibition (Jensen and Mazaheri, 2010; Mathewson et al., 2011; Klimesch, 2012; Iemi et al., 2022). Within these frameworks, it has been suggested that α rhythm determines the sampling rate of perception and the length of the time window within which two stimuli are temporally integrated (e.g., approximately 100 ms;

Samaha and Postle, 2015).

Overall, however, it remains unclear how pre-stimulus activity modulates performance in visual tasks. In particular, there is no consensus on whether α activity modulates unconscious sensory processing, aspects related to sensitivity or conscious access, or more general aspects of task performance. Moreover, nearly all existing studies have focused on very short-lived effects, in which pre-stimulus α activity influences perception of brief, static, and near-threshold stimuli. This approach cannot tell how long α activity can affect perceptual processing as the effects can only be determined within these short time windows. More importantly, tailored to isolate the role of α activity at a single point in time, this approach also ignores the dynamic nature of perception and the fact that the brain integrates information over hundreds of milliseconds before a conscious percept of the stimulus emerges (Sergent, 2018; Herzog et al., 2016, 2020).

To investigate the role of pre-stimulus α activity in long-lasting feature integration, we used here the sequential metacontrast paradigm (SQM; Otto et al., 2006; Otto et al., 2009). In the SQM, a central line is followed by pairs of flanking lines. When the central line contains

^{*} Corresponding author.

E-mail address: maelan.menetrey@gmail.com (M.Q. Menétrey).

<https://doi.org/10.1016/j.neuroimage.2023.120298>

Received 28 March 2023; Received in revised form 28 June 2023; Accepted 26 July 2023

Available online 29 July 2023

1053-8119/© 2023 The Author(s). Published by Elsevier Inc. This is an open access article under the CC BY license (<http://creativecommons.org/licenses/by/4.0/>).

a vernier offset, the offset is perceived at all lines (Fig. 1A). If a second offset, opposite to the central one, is later presented in the stream (the anti-vernier, Fig. 1A), the two offsets integrate and neither can be correctly reported. Critically, this integration occurs unconsciously and lasts up to 450 ms (Drissi-Daoudi et al., 2019; Herzog et al., 2020). This and similar long-lasting integration of visual features indicate that 1) conscious perception is substantially delayed relative to pre-stimulus brain activity, and that 2) unconscious integration can last much longer than a single α cycle.

Therefore, it is unknown today how existing findings on the role of pre-stimulus α rhythm in perception can generalize to the spatio-temporal feature integration that occurs in the SQM, covering several α cycles. One possibility is that α activity has no effect on this phenomenon, which would subsequently also call into question the effects observed on the integration of stimuli presented in periods of ~ 100 ms. Alternatively, α activity exerts a particular influence during unconscious processing, without being responsible for the integrative process *per se*. Indeed, because feature integration has been shown to be mandatory in the SQM (i.e., only the final integrated percept is accessible to consciousness; Drissi-Daoudi et al., 2019, 2021), any modulation of

performance related to α activity would imply an effect on how individual visual elements are weighted during unconscious sensory processing. One can also rule out the possibility that these effects act on high-level aspects of performance, such as response strategies or confidence, as there is no correct answer in the SQM when two opposite vernier offsets are presented.

To address this question, we used electroencephalography recordings (EEG) from previous work (Plomp et al., 2009). Participants reported the perceived offset direction in the SQM with either a single central vernier or this vernier and one anti-vernier (Fig 1B). Using the trials with two opposite verniers, we extracted pre-stimulus α power and phase in occipital electrodes where post-stimulus activity reflected the greater dominance of the 1st or 2nd offset. We found that α power, mediated by a slowing of the α frequency, affected the mutual performance of the two verniers, which were temporally separated by more than 100 ms. Thus, pre-stimulus α effects are not restricted to one cycle, arguing against cycles as time-keeper (Kononowicz and van Wassenhove, 2016) or periodic sampling (VanRullen, 2016b). Furthermore, given that feature integration in the SQM occurs before conscious perception is elicited (Drissi-Daoudi et al., 2019), our results provide

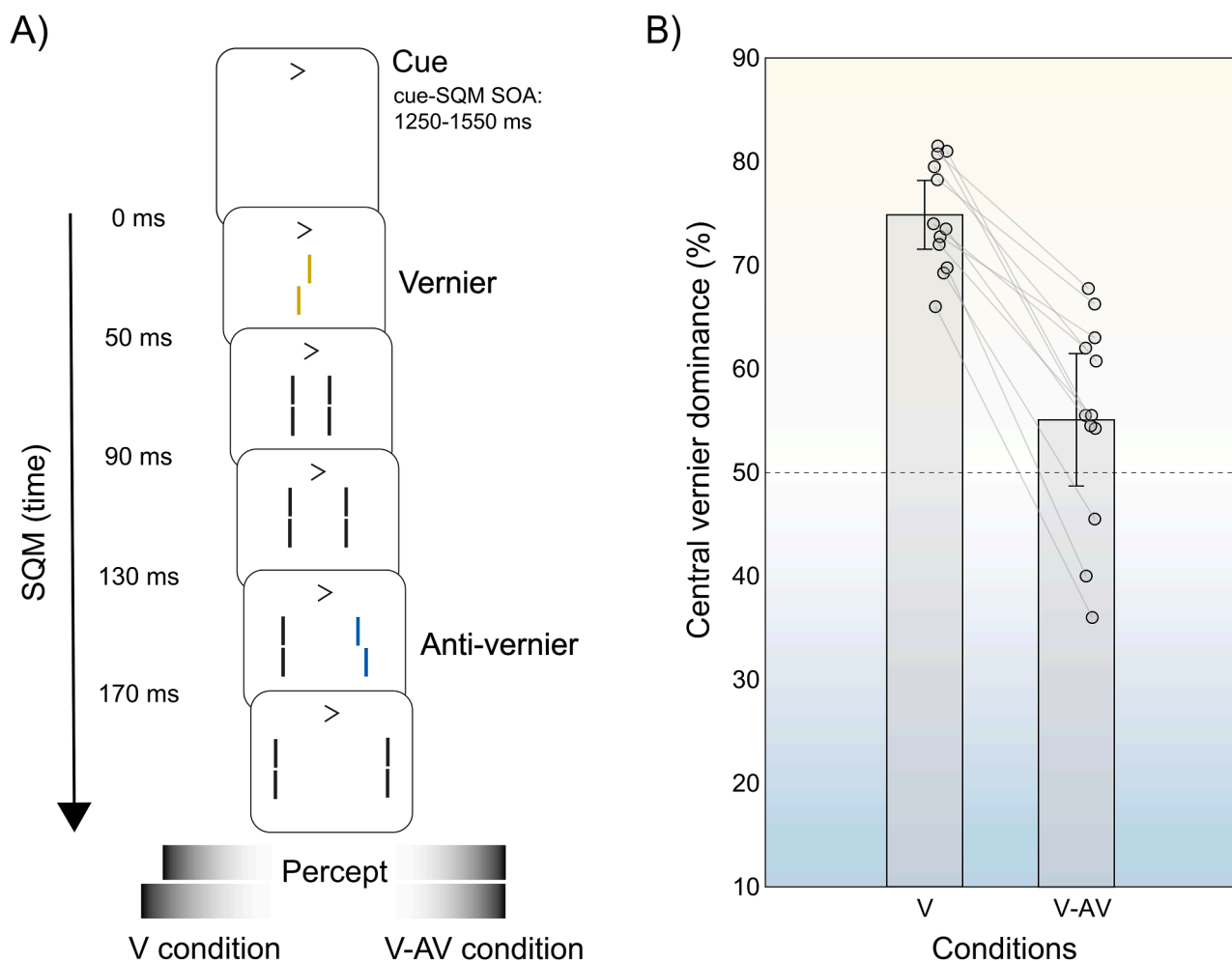


Fig. 1. A) In the sequential metacontrast paradigm (SQM), a central line is offset (i.e., a vernier) and is followed by a stream of lines that either contain only straight lines or one line with an additional offset in the opposite direction of the central vernier offset (i.e., called an anti-vernier). The SQM starts at a random interval (1250–1550 ms) after the presentation of a cue that directs attention to one of the two streams. Participants report the perceived offset at the end of the SQM (left vs. right). When only the central line is offset (i.e., the V condition), the offset appears at all lines, and offset discrimination performance is high. In the condition with two opposite verniers (i.e., the V-AV condition), the offsets cancel each other, and performance is around 50%. The yellow and blue verniers are used for illustrative purposes only, as all elements presented were white on a black background. B) Behavioral results from Plomp et al. (2009). A dominance level above 50% (yellow part of the graph) indicates that the central vernier offset dominates performance; a dominance level below 50% (blue part of the graph) indicates that the anti-vernier offset dominates performance. Circles indicate individual performances. The error bars represent the confidence interval of the mean (CI).

strong evidence that neural events in the α band are linked to mechanisms regulating unconscious sensory processing and affecting the relative weighting of individual features.

2. Methods

2.1. Participants, stimuli, and apparatus

We analyzed an existing dataset of EEG recordings with the SQM (Plomp et al., 2009). The dataset includes high-density event-related EEG from twelve healthy human participants. A detailed description of the stimuli, apparatus, and EEG acquisition can be found in the original manuscript (Plomp et al., 2009).

Participants were presented with a central offset line (i.e., a vernier) followed by 4 pairs of lines, propagating on both sides (Fig. 1A). All pairs of lines were straight except for the third pair, shown 110 ms after the central vernier, which presented one straight line and one line with an offset in the opposite direction to the central vernier offset (i.e., an anti-vernier). The central line consisted of two segments of 10' (arcminute) length separated by a vertical gap of 1'. The length of the first pair of lines was 11.6' and increased progressively by 1.6' for the following pairs. The horizontal distance from the center increased progressively by 3.2' with each pair of lines.

At the beginning of each trial, a cue indicated the relevant side (left or right) of the stream that participants had to attend to. The cue was presented at 0.5° above the location of the SQM and remained on screen for the entire trial duration. After the onset of the cue, the central line was presented at a random interval between 1250 and 1550 ms. In half of the trials, participants attended to the stream containing the two opposite vernier offsets.

Each element of the SQM was presented for 20 ms, with blank intervals of 30 ms (between the central vernier and the first pair of lines) and 20 ms (between all the other pairs). The total sequence lasted 190 ms. Participants had to report the perceived offset in the cued stream —i.e., whether the lower segment was offset to the left or right compared to the upper segment of the vernier. The size of the central vernier offset was calibrated before the experiment to achieve 75% of discrimination accuracy (mean size = 1.72'; SD = 0.4'), in the absence of an anti-vernier. Similarly, the size of the anti-vernier was calibrated to achieve equal dominance when presented after the central vernier (mean size = 0.83'; SD = 0.22').

The main conditions of interest are referred to as *vernier only* (V condition) when participants attended to a stream with no anti-vernier, and *vernier anti-vernier* (V-AV condition) when participants attended to a stream containing also an anti-vernier. The experiment consisted of 800 trials in total (10 blocks of 80 trials).

2.2. EEG preprocessing

Details on the raw EEG data can be found in the original manuscript (Plomp et al., 2009). EEG data were preprocessed using Matlab (version R2018b, The MathWorks Inc., Natick, USA) and EEGLAB (version v2021.1; Delorme and Makeig, 2004; Delorme et al., 2011), using 160 out of 192 electrodes, according to the Biosemi standard 160 template. Data were downsampled to 256 Hz and re-referenced to the robust average reference using *prepline* (Bigdely-Shamlo et al., 2015), which also provided an estimate of outlier electrodes (correlation criterion, threshold of 0.2). Data were then detrended at <1 Hz (de Cheveigné and Arzounian, 2018), epoched from -1.5 s to 1.5 s relative to the onset of

the central vernier, and cleaned from line noise via spectrum interpolation (Leske and Dalal, 2019). A two-step ICA (FastICA; Hyvärinen and Oja, 2000) was used to reject bad epochs (*pop_jointprob.m*, global threshold: all-electrodes grouped = 2 SD), and to isolate other physiological artifacts. The “bad” independent components, labeled by crossing machine-learning routines (MARA, Multiple Artifact Rejection Algorithm in EEGLAB; Winkler et al., 2011, 2014) with the criterion of >90% of total variance explained, were removed manually (Pascucci et al., 2020). The “bad” electrodes were then interpolated using the nearest-neighbor spline method and data were re-referenced again to the average reference. In total, 4.68% of the electrodes were interpolated, while 5.02% of the epochs and 20.31% of the independent components were removed.

2.3. EEG decoding

We used linear discriminant analysis (LDA) to decode the reported (and perceived) offset from the evoked EEG scalp topographies. We implemented LDA with custom-made functions written in Matlab, based on the recommended settings for EEG data (Subasi and Gursoy, 2010; Grootswagers et al., 2017). A two-fold cross-validation routine was reiterated 500 times, sampling 80% of the trials at each iteration and combining them into pseudo-trials (an average of 8 trials each). Testing and training sets were z-scored to the distribution of the training set and the decoder weights were estimated using a regularized covariance (Ledoit and Wolf, 2004; Haufe et al., 2014; Kayser et al., 2016). The decoder weights from the training set were used to predict the classes —i.e., the reported offset, from the EEG data in the testing set. The area under the curve (AUC) was taken as the performance measure. This procedure was performed for each time point, from -100 to 1000 ms, using a sliding window of 17 samples which corresponds to a resolution of 66.4 ms (Grootswagers et al., 2017). A surrogate performance metric was also created by randomly shuffling the labels of the testing classes and computing surrogate AUC values 1000 times.

In the main analysis, LDA was used to classify the reported offset in trials where participants attended to the stream containing both the vernier offsets (V-AV trials). The decoder discriminated whether participants' reports were related to the central vernier offset (*1st reported offset*) or to the anti-vernier offset (*2nd reported offset*; Fig. 2A). As control analyses, we followed the same procedure to discriminate reports of the vernier offset in V trials (*correct vs. incorrect*; see Supplementary Fig. 1A), as well as to discriminate correct reports in V trials from reports of the 1st or 2nd offset in V-AV trials (Fig. 2B).

The statistical assessment of the decoding results was performed using cluster-based permutation approaches and surrogate analysis (Nichols and Holmes, 2002; Maris and Oostenveld, 2007; Kayser et al., 2016). Clusters were defined as consecutive time points in which the decoder results were significantly higher than chance (chance = 0.5, paired *t*-test with $\alpha = 0.05$). The sum of *t*-values within each cluster was then compared against the maximum of the sum obtained from surrogate clusters (number of permutations = 10,000). Significant time points corresponded to clusters with a probability of <0.05 in the surrogate data.

To identify electrodes sensitive to the difference between classes, we estimated activation patterns from the LDA decoder (Haufe et al., 2014; Grootswagers et al., 2017, 2018; Park and Kayser, 2019). After averaging activation patterns across the significant decoder windows and participants, we selected the electrodes whose absolute activation signal was above the 95th quantile. The single-trial average activity in these

electrodes (A11, A12, A23, A24, A25, A26, A27, A28) was then used for time-frequency pre-stimulus analysis.

2.4. Time-frequency analysis

Focusing on the subset of electrodes derived from the LDA, a time-frequency representation of the instantaneous power and phase was obtained using the Morlet Wavelet Transform (width = 7; Tallon-Baudry, 1999). The frequencies of interest (from 4 to 20 Hz in steps of 0.5) corresponded to a wide range around the α band oscillations, in line with previous studies (e.g., van Dijk et al., 2008; Busch et al., 2009). We separately analyzed the power and phase in the pre-stimulus interval to investigate their relationship with the reported offset in V-AV trials.

In the analysis of power, for each frequency and time point of interest (from -500 to -100 ms), we applied a multilevel linear model (Frömer et al., 2018) to predict fluctuations in pre-stimulus power as a function of the reported offset (1st vs. 2nd). The model included an intercept and the 'report' predictor as fixed effects, and a random intercept accounting for inter-individual shifts in the average power level. The resulting regression coefficients with related t -values and p -values, were stored in a time-frequency matrix (see Fig. 3A). P -values in the time-frequency matrix were corrected for multiple comparisons using the false discovery rate method (FDR; Storey, 2002). We repeated the power analysis with reports in the V trials (correct vs. incorrect; see Supplementary Fig. 1C).

In the analysis of phase, we followed the procedure suggested by VanRullen (2016a): First, inter-trial phase coherence (ITC; also called phase-locking factor) was computed to measure the phase synchronization across trials of each class (1st vs. 2nd reported offset) as well as across all trials, independently of the class (Tallon-Baudry et al., 1996). Second, the Phase Opposition Sum index (POS) was calculated to assess whether the phase distribution across trials of each class was random, phase-locked to the same angle, or to different angles (VanRullen, 2016a). Third, a non-parametric permutation procedure combining permutation and z -score tests was performed to statistically evaluate the POS index (VanRullen, 2016a). As a final step, p -values at each time and frequency point were corrected for multiple comparisons using the false discovery rate correction (FDR; Storey, 2002) and converted into t -values.

Lastly, we investigated the relationship between the significant pre-stimulus α cluster found in the power analysis (see Fig. 3A) and the instantaneous α frequency, following the procedure proposed by Cohen (2014). To estimate fluctuations of the instantaneous α frequency, the signal was first bandpass filtered within the range of the significant cluster found in pre-stimulus α power (10.5 to 12.5 Hz). Second, the instantaneous phase angle over time was estimated using the Hilbert transform and the instantaneous α frequency was derived from the time rate at which the instantaneous phase angle changes (i.e., the temporal derivative of the instantaneous Hilbert phase, scaled by the sampling rate and $2^*\pi$). Third, as the noise in the phase angle time series might lead to abrupt changes in its derivative, a median filter was additionally applied to the instantaneous frequency estimate (10 equally spaced windows of 400 ms, see Cohen, 2014) and the instantaneous α frequency for each subject was calculated from the estimated median instantaneous frequency for all median-filter windows and all electrodes.

Driven by the results of the power analysis, we further explored, post-hoc, differences in the instantaneous α frequency between trials

with 1st vs. 2nd reported offset, using a cluster-based permutation test (Nichols and Holmes, 2002; Maris and Oostenveld, 2007). Clusters were defined as consecutive time points in which the difference between the two conditions was significantly different from 0 (paired t -test with $\alpha = 0.05$; see Fig. 4A). Using RStudio 2022.02.0 (R Core Team, 2022), a mediation analysis was also performed to determine whether instantaneous α frequency (converted into z -scores) mediates the relationships between pre-stimulus α power (linearized with log-transformation and converted into z -score) and reported offset (1st vs. 2nd; see Fig. 4B). To this end, a general linear model was first applied to compute the total effect of pre-stimulus α power on the reports. Second, a linear regression was performed to examine the relationship between α power and instantaneous α frequency. Third, to confirm the mediating role of instantaneous α frequency, we applied a general linear model while controlling for α power. The R package "medflex" was used to estimate direct and indirect effects (Steen et al., 2017).

3. Results

In the V-AV condition of the SQM, two opposite vernier offsets are integrated and only a small offset or no offset is consciously perceived (Fig. 1B). Even though participants show a slight dominance in their responses for the first or second vernier, integration still occurs unconsciously, i.e., the verniers cannot be reported separately (Herzog et al., 2016; Drissi-Daoudi et al., 2019).

As mentioned earlier, we focused on the analysis of EEG data in V-AV trials, following two steps. First, we used a linear classifier to decode the offset reported in V-AV trials from post-stimulus EEG activity. Second, we looked at the influence of pre-stimulus oscillations on the SQM, focusing on the most relevant electrodes from the decoder results. All analyses were time-locked to the onset of the SQM, i.e., the presentation of the central vernier. Because of the long interval between cue and SQM onset (1250–1550 ms), it is unlikely that our pre-stimulus windows are contaminated by cue-related neural responses.

3.1. Decoding the reported offset from post-stimulus EEG activity

We used LDA to decode V-AV trials where participants reported the 1st (central vernier) or the 2nd (anti-vernier) offset (see Methods). The LDA successfully discriminated the reported offset in a time window from 340 ms to 960 ms after the onset of the SQM (cluster-based permutation test, $p < .05$, Cohen's $d = 2.26$; Fig. 2A). The decoder topography (e.g., the activation patterns; Haufe et al., 2014) revealed a stronger contribution of posterior electrodes throughout the entire significant window (Fig. 2D). Hence, post-stimulus EEG activity patterns discriminated whether participants reported the 1st or 2nd offset, well before the actual behavioral report (averaged reaction times in V-AV trials = 899 ms).

As a control, we obtained similar decoding results when LDA classified the correct reports of the central vernier offset in V trials (i.e., trials with only the central vernier offset) from the reports of the 2nd offset in V-AV trials (cluster-based permutation test, $p < .05$, Cohen's $d = 1.81$; Fig. 2B). Conversely, LDA was unable to discriminate the correct reports in V trials from the reports of the 1st offset in V-AV trials (Fig. 2B), indicating that the decoder results were largely driven by the presence, and report, of the anti-vernier.

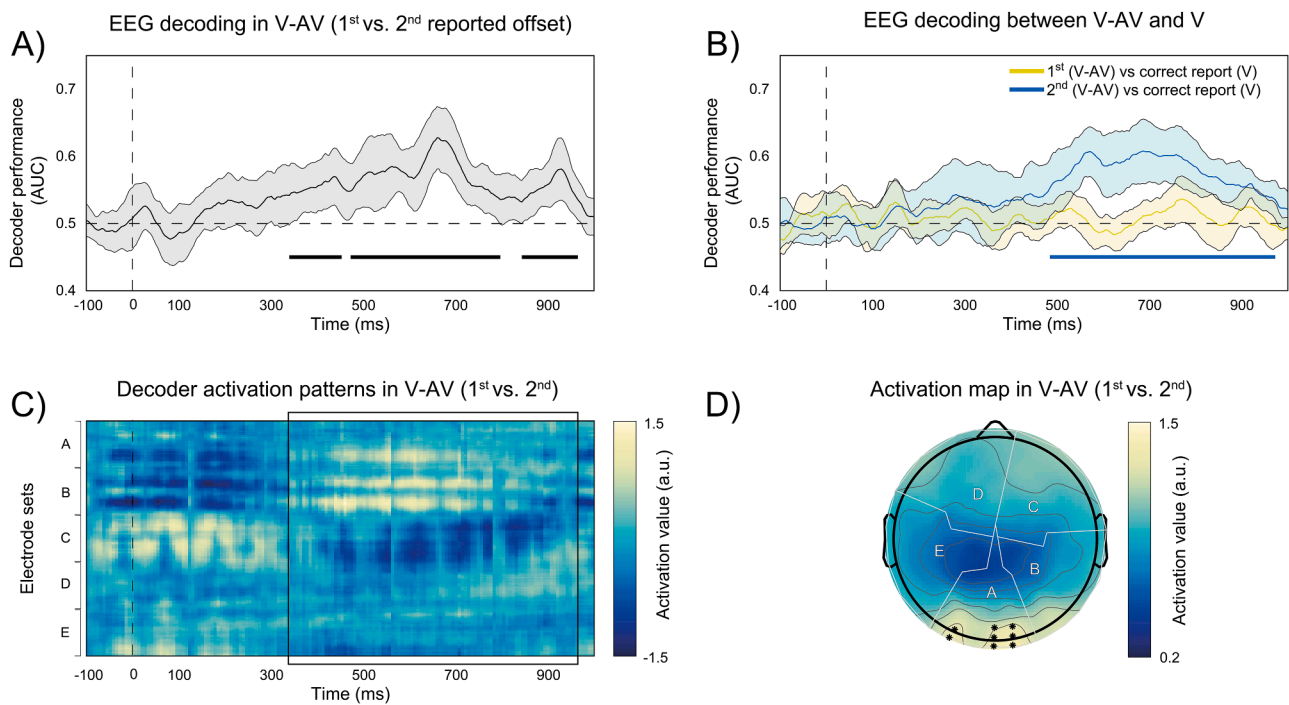


Fig. 2. A) EEG decoding results in V-AV trials. LDA discriminates the reported offset above chance (1st or 2nd; group average AUC and 95% CI). Significant time windows are highlighted by the black horizontal lines (AUC above 0.5, cluster-based permutation test, $p < .05$, Cohen's $d = 2.26$). B) EEG decoding results in V-AV vs. V trials. LDA successfully discriminates the report of the 2nd offset in V-AV trials from the correct report of the central vernier offset in V trials (in blue, group average AUC and 95% CI). Significant time windows are highlighted by the blue line (AUC above 0.5, cluster-based permutation test, $p < .05$, Cohen's $d = 1.81$). In contrast, LDA was unable to discriminate the report of the 1st offset in V-AV trials from the correct report of the central vernier offset in V trials (in yellow, group average AUC and 95% CI). C) Activation patterns derived from the decoding results in V-AV trials for each electrode, averaged across participants. The significant time window is indicated by a black rectangle. D) Topography of the activation patterns derived from the decoding results in V-AV trials, averaged across the entire significant window and participants. Sections and letters indicate the standard Biosemi 160-electrode arrangement. Asterisks show the subset of electrodes whose absolute activation is above the 95th quantile.

3.2. Pre-stimulus α oscillations influence the reported offset

In the second step, we focused on the subset of occipital electrodes showing larger discriminant post-stimulus activity (Fig. 2D). We investigated whether the activity at these electrodes can also affect the reported percept before the stimulus has even occurred. To this aim, we compared pre-stimulus spectral power and phase between V-AV trials in which participants reported the 1st or 2nd vernier offset.

In the analysis of pre-stimulus power, a multilevel linear model (see Methods) revealed a significant effect in the α range (10.5 to 12.5 Hz) with a peak around -350 ms (from -456 to -260 ms). This effect was consistent with an increase in pre-stimulus α power when participants reported the 1st vernier offset (Fig. 3A). Because pre-stimulus α activity is known to change over the course of an experiment (Benwell et al., 2019), we confirmed the results also after controlling for trial order (see Supplementary Material). Moreover, this effect only occurred in V-AV trials where participants attended to the stream with both the central vernier and the anti-vernier. No relationship between α power and the reports was evident in V trials, i.e., trials where no anti-vernier was presented (see Supplementary Fig. 1C).

At the pre-stimulus latencies of this effect (Fig. 3A), there was a clear increase in α power when the 1st vernier offset was reported, and a clear reduction when the 2nd offset was reported (Fig. 3C, $t(11) = 3.75$, $p = .003$, Cohen's $d = 1.08$, 95% CI (0.04, 0.17)). The topographies of the effect revealed a marked increase in α power at occipital sites when the 1st offset was reported (Fig. 3D).

In the analysis of pre-stimulus phase, the POS (see Methods) revealed no consistent phase-locking opposition as a function of the reported

offset —i.e., differences in pre-stimulus phase, at any frequency, were unrelated to the final report (Fig. 3B).

3.3. Power increases are followed by the slowing of α rhythm

Our analysis of pre-stimulus power revealed effects in the α band from ~ 300 ms before the SQM. Since previous studies have shown that changes in α activity affect perception of brief stimuli occurring immediately after or within short time scales (Busch et al., 2009), it is unclear how these peaks far back in time can influence processing in the SQM. One possibility is that α peaks produce longer-lasting changes in neural activity that are not limited to the peak itself but, in this paradigm, extended to the beginning of the SQM and influenced how the 1st vernier was processed and integrated into the stream. Several studies have shown that increases in α power are followed by the slowing of the α rhythm, which may eventually provide longer periods of reduced inhibition of sensory input (Atallah and Scanziani, 2009; Himmelstoss et al., 2015; Samaha and Postle, 2015; Klimesch, 2018; Sharp et al., 2022). If this were the case, trials where participants reported the 1st offset should exhibit a slowing of the α frequency at the beginning of the stream, compared to trials on which participants reported the 2nd offset. We explored this possibility with a post-hoc analysis, by estimating the instantaneous α frequency with the method proposed by Cohen (2014; see Methods). The EEG signal at the occipital electrodes selected for the pre-stimulus analysis (see “Pre-stimulus α oscillations influence the reported offset”) was first filtered in the 10.5–12.5 Hz band, corresponding to the significant band of α power effects found (Fig. 3A). We then computed the instantaneous α frequency in a time window covering

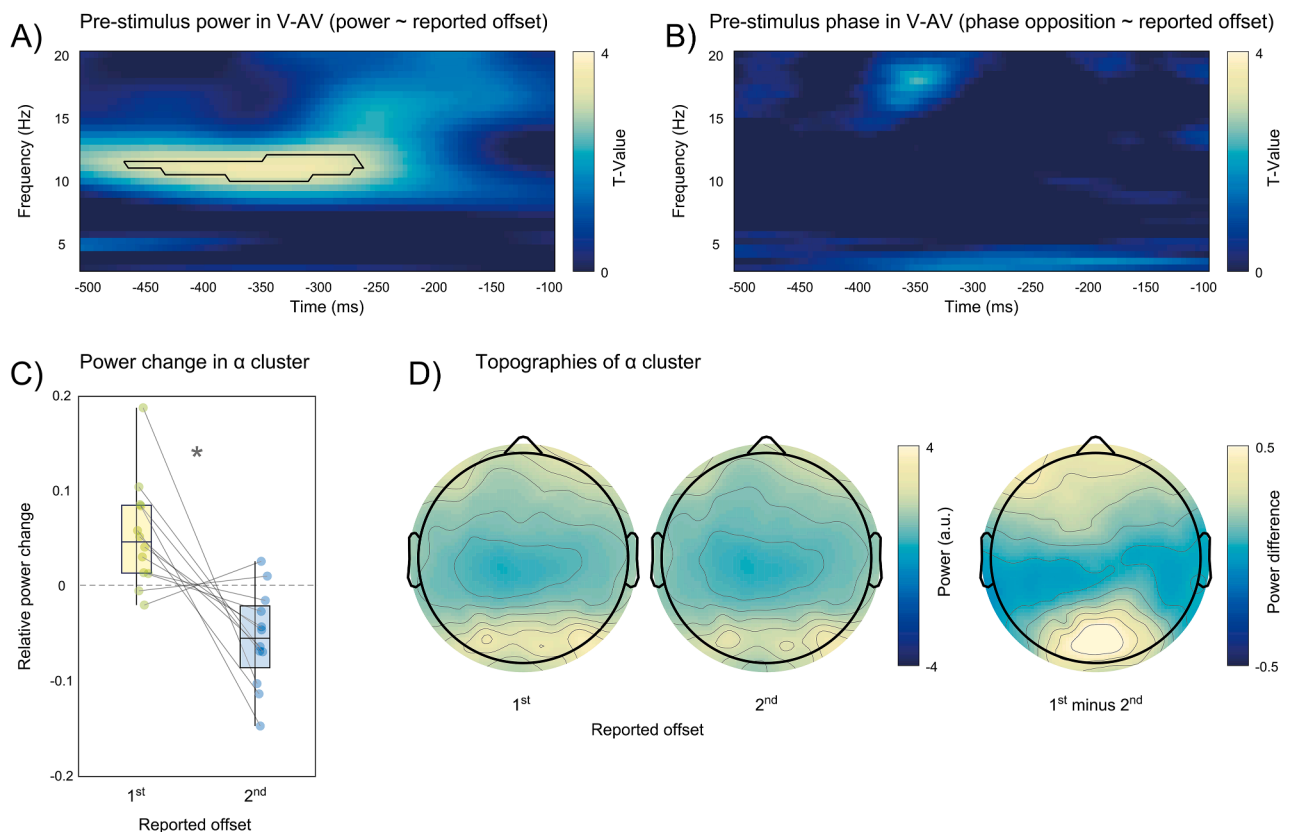


Fig. 3. A) Pre-stimulus power analysis in V-AV trials. Results from the linear mixed model predicting the relationship between pre-stimulus EEG power and the reported offset (1st or 2nd). A significant cluster in the α band is highlighted by the black line ($p < .05$, FDR). B) Pre-stimulus phase analysis in V-AV trials. Phase Opposition Sum index (POS) evaluates the relationship between phase distribution and the reported offset (1st or 2nd). No significant effect was found (permutation and z-score tests, $p < .05$, FDR). C) Power change in the significant pre-stimulus power cluster as a function of the reported offset. Power changes are computed relative to the mean power across all trials in V-AV trials. The asterisk indicates a significant difference ($p = .003$, Cohen's $d = 1.08$). Circles indicate individual power change. The error bars represent the confidence interval of the mean (CI). D) Topographies of the significant pre-stimulus power cluster as a function of the reported offset and topography of power differences (1st reported offset minus 2nd reported offset).

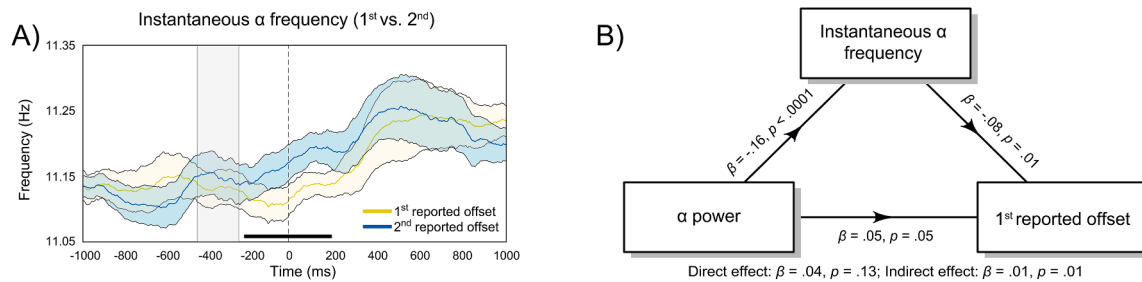


Fig. 4. A) Instantaneous α frequency in V-AV trials as a function of the reported offset (1st vs. 2nd; respectively in yellow and blue, 95% CI). Significant differences are highlighted by the black line (cluster-based permutation test, $p < .05$, Cohen's $d = 1.25$). The time window of the significant pre-stimulus α cluster is indicated by the gray-shaded area. B) Mediation analysis. Instantaneous α frequency fully mediates the relationship between α power and reported offset (1st vs. 2nd; Indirect effect: $\beta = 0.01 \pm 0.004$, $p = .01$).

both pre- and post-stimulus intervals and compared V-AV trials in which participants reported the 1st or the 2nd vernier offset. The results of this analysis revealed a significant difference in instantaneous α frequency from -230 ms before to 168 ms after the SQM onset (cluster-based permutation test, $p < .05$, Cohen's $d = 1.25$; Fig. 4A), with a lower frequency around the time of stimulus presentation when the 1st offset was reported. Note that the instantaneous α frequency can be confounded by differences in the slope of the power spectrum ($1/f$ activity; Samaha and Cohen, 2022). That is, when $1/f$ activity is high and α power is low, the method of frequency sliding can underestimate the true frequency of the signal. This confound, however, cannot be the cause of our results, since we found that the instantaneous α frequency decreases, rather than increases, hundreds of milliseconds after α rises in power. Additional analysis correcting for $1/f$ activity further confirmed this finding (see Supplementary Fig. 2).

To disentangle whether the pre-stimulus α power effect on participants' reports was mediated by the slowing of the α rhythm and not the main cause, we next performed a mediation analysis (see Fig. 4B), with single-trial α power as the independent variable, the single-trial instantaneous α frequency in the significant time window as the mediator, and the participants report as the dependent variable (1st or 2nd offset; see Methods for the details on the mediation model). This analysis confirmed that increases in pre-stimulus α power were followed by decreases in the instantaneous α frequency ($\beta = -0.16 \pm 0.01$, $p < .0001$), and that the instantaneous α frequency fully mediated the relationship between pre-stimulus α power and reported offsets (Indirect Effect: $\beta = 0.01 \pm 0.004$, $p = 0.01$). While lower instantaneous α frequency increases the probability of reporting the 1st vernier offset ($\beta = -0.08 \pm 0.03$, $p = 0.01$), α power effects are no longer significant when mediated by the instantaneous α frequency variable ($\beta = 0.04 \pm 0.03$, $p = .13$). It may be argued that α power and frequency slowing reflect the same process, thus, the mediation results would only be redundant. However, even though α power was a strong predictor of the subsequent frequency slowing, not all the variance in one variable was explained by the other (R^2 of a model predicting instantaneous α frequency with α power = 0.02 , $F(1,4575) = 117.7$, $p < .0001$). Hence, trial-by-trial fluctuations in α power and instantaneous frequency could still be informative in the context of mediation analysis.

4. Discussion

In this study, we investigated the role of pre-stimulus α rhythm during long-lasting feature integration. We analyzed EEG recordings during the SQM paradigm, where two vernier offsets embedded in a rapid stream of lines are integrated into a single percept (Otto et al., 2006; Otto et al., 2009). A two-step procedure was followed for the analyses. First, using a linear classifier we decoded the offset that participants reported in trials with two opposite vernier offsets. This revealed topographies and electrodes where post-stimulus activity reflected the dominance of the 1st or 2nd vernier in the final conscious

percept, needed to confirm that feature integration in the SQM is not always uniform. Second, we analyzed pre-stimulus activity at these specific electrodes, covering the occipital area.

We found that pre-stimulus α power, but not phase, can influence the unconscious processing of two opposite vernier offsets in the SQM stream. Higher pre-stimulus α power, occurring even 300 ms before the stimulus, leads to more responses related to the central vernier offset, while lower power leads to more responses related to the anti-vernier offset. These peaks in α power are followed by a relatively long-lasting slowing of the α frequency, extending to the beginning of the SQM, and likely providing longer windows of reduced inhibition that increased the contribution of the 1st vernier in the unconscious integration process. Because the two verniers integrate before a conscious percept is elicited (Drissi-Daoudi et al., 2019), our findings indicate that pre-stimulus α power affects the relative weighting of individual features during unconscious feature integration.

Our findings are important for two main reasons. First, we show that the percept resulting from the long-lasting unconscious feature integration of the SQM can be decoded from post-stimulus EEG activity. Second, we demonstrate that pre-stimulus brain activity can affect unconscious feature integration not simply because of a transitory event (e.g., a peak in power) but as a result of a cascade of neural changes.

As for the first point, previous research has shown that differences between trials with a single vernier (V trials) or two opposite verniers (V-AV trials) become evident only during later stages of decision-making and response-related processing (e.g., from around 650 to 250 ms before the motor response), suggesting that feature integration is a top-down process and the resulting conscious percept is timed endogenously (Plomp et al., 2009). Here, we found that the dominance of one of the two vernier offsets in V-AV trials is reflected by neural activity patterns timed to the stimulus and well before the response. Using a linear classifier, we showed that post-stimulus EEG activity discriminates whether participants will report the offset of the central vernier or the one of the anti-vernier. The reported offset was decodable from around 350 milliseconds after the stimulus onset (Fig. 2A), with a strong contribution from occipital electrodes (Fig. 2C/D), likely reflecting ongoing visual processing before the final integrated conscious percept emerges. Importantly, the power of α rhythm at the same electrodes was predictive of the reported offset already hundreds of milliseconds before the stimulus was even presented (Fig. 3A).

As for the second point, pre-stimulus modulations of α power, which generally coincide with attention, task engagement, and vigilance (Sauseng et al., 2005; Kelly et al., 2006; Samaha et al., 2016), have been linked to various phenomena in perception, including changes in visual sensitivity (Brüers and VanRullen, 2018; Zhou et al., 2021; Michail et al., 2022) and modulations of high-level aspects of performance such as response criterion (Limbach and Corballis, 2016), perceptual awareness (Benwell et al., 2017), or subjective confidence (Samaha et al., 2017). However, these effects cannot explain why higher pre-stimulus α power leads to more reports of the first vernier offset in the SQM. In this

paradigm, the integration of the two offsets is mandatory and occurs before conscious awareness. Even when participants are informed about the paradigm and the number of verniers presented, they are unable to segregate two verniers separated by 330 ms, i.e., they cannot report the vernier offsets independently, for example, one by one (Drissi-Daoudi et al., 2019). Additionally, there are no correct responses in V-AV trials, thus, shifts in response criterion or subjective confidence cannot affect performance. Participants exhibit chance performance on average, which is solely attributed to the presentation of both the vernier and the anti-vernier within the same stream (Otto et al., 2010).

On the other hand, several studies have shown that α phase can be linked to two aspects of perception: periodic cycles of perceptual processing and temporal windows of integration (Wutz et al., 2014; VanRullen, 2016b; Ronconi et al., 2017; Fakche and Dugué, 2022). First, periodic cycles in perception suggest that the phase of an α cycle determines the probability of detecting a visual stimulus, with stimuli at optimal phases leading to higher hit rates and those at opposite phases leading to higher miss rates (Busch et al., 2009; Mathewson et al., 2009). Second, temporal integration windows suggest that integration is constrained within a cycle of α activity, with integration occurring only when two stimuli fall within the same α cycle (Varela et al., 1981; VanRullen, 2016b; Lundqvist and Wutz, 2022). However, we did not find a systematic relationship between α phase and the reported offset in the SQM (Fig. 3B). These findings add to the ongoing debate about the generalizability and robustness of phase effects in perception (Ruzzoli et al., 2019; Benwell et al., 2022; Keitel et al., 2022). In addition, the long-lasting integration in the SQM extends beyond three α cycles (Drissi-Daoudi et al., 2019), making it incompatible with windows lasting only a single α cycle. We have recently pointed out that clear links between α effects and specific aspects of perception need to be established, notably whether α activity affects the content or the temporal structure of consciousness (Menétrey et al., 2022). Here, we suggest that α activity modulates sensory representation (Zhou et al., 2021) during unconscious processing, without being involved in sampling or integration *per se*.

Our results demonstrate that neither the phase nor changes in the power alone can explain the influence of pre-stimulus α activity in long-lasting feature integration. Indeed, our results indicate that the effect of α power was mediated by a subtle but significant decrease in the instantaneous α frequency when the 1st vernier was reported. This finding is in line with evidence that peaks in α power mark the beginning of a cascade of neural changes, leading to the temporary slowing of α oscillations (Klimesch, 2018). Slower α rhythm might lengthen the ‘duty cycle’ (Peylo et al., 2021), or the excitatory part of a neural oscillation’s cycle, which in our paradigm, may have overlapped with the time of the central vernier, leading to its enhanced processing and dominance in feature integration. Thus, slower α frequencies facilitate the responsiveness of neurons to weak or brief stimuli, whereas faster α frequencies offer greater precision but neurons are less readily triggered (Cohen, 2014). This process may occur over longer time scales, explaining why the effects of α phase and power are often found well before the stimulus onset and persist beyond a single α cycle (e.g., Busch et al., 2009; Zazio et al., 2022). These results, obtained with visual stimuli only, add to other findings demonstrating that pre-stimulus α activity predisposes perceptual integration in multisensory paradigms (Leonardelli et al., 2015; London et al., 2022).

A potential limitation of this work is the small sample size, due to the sample collected in the original study (Plomp et al., 2009). Nevertheless, the large effect size reported in the effect of pre-stimulus α power (e.g., Cohen’s $d = 1.08$), even if with only twelve participants, sets a promising starting point for future research.

Lastly, a key question is whether these changes in α power, which eventually lead to the slowing of the α rhythm, reflect purely spontaneous fluctuations or events induced by other factors, such as modulations of attention and expectations (Bauer et al., 2014; Sanders et al., 2014; Cao et al., 2017; Michalareas et al., 2016; Grabot et al., 2021). For

instance, participants may have expected to see an offset from the beginning of the stream, because they can easily see it in half of the trials (V condition). Hence, in some trials they may have focused more on the central offset, enabling pre-stimulus attentional mechanisms to inhibit the motion stream (Sauseng et al., 2005; Thut, 2006; Foxe and Snyder, 2011; Pascucci et al., 2018; Pagnotta et al., 2020, 2022). Predictive coding frameworks also propose that perception is a process of inference that combines bottom-up sensory inputs and top-down expectations (Friston, 2005). According to this perspective, expectations can generate pre-activations of stimulus representations (Kok et al., 2017), which ultimately exert an influence on sensory processing (Kok et al., 2012) or decision-making (Hesselmann et al., 2008a, 2008b). Notably, these effects may be implemented via top-down signals in the α band (Peylo et al., 2021). Alternatively, a recent view proposes a relationship between α power and oculomotor control, in which high α power corresponds to reduced gaze variability (Jensen et al., 2021; Popov et al., 2021; Pan et al., 2022). Under this view, one can also hypothesize that the increases in pre-stimulus α power were due to a decreased tendency to saccade towards the cued side of the stream.

5. Conclusion

To make sense of the dynamic world around us, the brain must integrate visual information over hundreds of milliseconds. Motion perception is just one example. Here, we show that modulations of α activity can induce long-lasting changes in neural activity that affect the way visual features are integrated into the conscious percept. In particular, we found that pre-stimulus α power can affect feature integration over long windows of time. We did not find any phase effects in this integration process. We propose that α power increases lead to a transient lengthening of the duty cycles in subsequent α cycles, thus, enhancing the representation of the central vernier offset in the integrated percept. These findings illustrate the existence of flexible and cascade-like mechanisms governed by α activity that can influence the relative contribution of features in a stream. In addition, they provide support for a role of α activity in determining the unconscious processing of features before the conscious percept emerges, rather than simply modulating the perception of a static stimulus.

Data availability

EEG and behavioral data are available on the Open Science Framework (<https://osf.io/7x8hc/>). Additional data related to this paper may be requested from the corresponding author.

CRediT authorship contribution statement

Maëlan Q. Menétrey: Conceptualization, Methodology, Formal analysis, Investigation, Data curation, Writing – original draft, Visualization. **Michael H. Herzog:** Writing – review & editing, Supervision, Resources, Funding acquisition. **David Pascucci:** Conceptualization, Methodology, Formal analysis, Investigation, Writing – review & editing, Funding acquisition.

Declaration of Competing Interest

The authors declare no competing financial interests.

Acknowledgments

We would like to thank Gijs Plomp for collecting the data and giving us the opportunity to analyze them. This work was supported by the Swiss National Science Foundation (grant number 325130_204898, ‘Basics of visual processing: the first half second’; grant numbers PZ00P1_179988 and PZ00P1_179988/2).

Supplementary materials

Supplementary material associated with this article can be found, in the online version, at [doi:10.1016/j.neuroimage.2023.120298](https://doi.org/10.1016/j.neuroimage.2023.120298).

References

- Adrian, E.D., Matthews, B.H.C., 1934. The Berger rhythm: potential changes from the occipital lobes in man. *Brain* 57 (4), 355–385. <https://doi.org/10.1093/brain/57.4.355>.
- Allallah, B.V., Scanziani, M., 2009. Instantaneous modulation of gamma oscillation frequency by balancing excitation with inhibition. *Neuron* 62 (4), 566–577. <https://doi.org/10.1016/j.neuron.2009.04.027>.
- Bauer, M., Stenner, M.-P., Friston, K.J., Dolan, R.J., 2014. Attentional modulation of alpha/beta and gamma oscillations reflect functionally distinct processes. *J. Neurosci.* 34 (48), 16117–16125. <https://doi.org/10.1523/JNEUROSCI.3474-13.2014>.
- Benwell, C.S.Y., Coldea, A., Harvey, M., Thut, G., 2022. Low pre-stimulus EEG alpha power amplifies visual awareness but not visual sensitivity. *Eur. J. Neurosci.* 55 (11–12), 3125–3140. <https://doi.org/10.1111/ejn.15166>.
- Benwell, C.S.Y., London, R.E., Tagliabue, C.F., Veniero, D., Gross, J., Keitel, C., Thut, G., 2019. Frequency and power of human alpha oscillations drift systematically with time-on-task. *Neuroimage* 192, 101–114. <https://doi.org/10.1016/j.neuroimage.2019.02.067>.
- Benwell, C.S.Y., Tagliabue, C.F., Veniero, D., Cecere, R., Savazzi, S., Thut, G., 2017. Prestimulus EEG power predicts conscious awareness but not objective visual performance. *eNeuro* 4 (6). <https://doi.org/10.1523/ENEURO.0182-17.2017>.
- Bigdely-Shamlo, N., Mullen, T., Kothe, C., Su, K.-M., Robbins, K.A., 2015. The PREP pipeline: standardized preprocessing for large-scale EEG analysis. *Front. Neuroinform.* 9 <https://doi.org/10.3389/fninf.2015.00016>.
- Bishop, G.H., 1932. Cyclic changes in excitability of the optic pathway of the rabbit. *Am. J. Physiol.-Legacy Content* 103 (1), 213–224. <https://doi.org/10.1152/ajplegacy.1932.103.1.213>.
- Brüers, S., VanRullen, R., 2018. Alpha power modulates perception independently of endogenous factors. *Front. Neurosci.* 12, 279. <https://doi.org/10.3389/fnins.2018.00279>.
- Busch, N.A., Dubois, J., VanRullen, R., 2009. The phase of ongoing EEG oscillations predicts visual perception. *J. Neurosci.* 29 (24), 7869–7876. <https://doi.org/10.1523/JNEUROSCI.0113-09.2009>.
- Cao, L., Thut, G., Gross, J., 2017. The role of brain oscillations in predicting self-generated sounds. *Neuroimage* 147, 895–903. <https://doi.org/10.1016/j.neuroimage.2016.11.001>.
- Cohen, M.X., 2014. Fluctuations in oscillation frequency control spike timing and coordinate neural networks. *J. Neurosci.* 34 (27), 8988–8998. <https://doi.org/10.1523/JNEUROSCI.0261-14.2014>.
- de Cheveigné, A., Arzounian, D., 2018. Robust detrending, rereferencing, outlier detection, and inpainting for multichannel data. *Neuroimage* 172, 903–912. <https://doi.org/10.1016/j.neuroimage.2018.01.035>.
- Delorme, A., Makeig, S., 2004. EEGLAB: an open source toolbox for analysis of single-trial EEG dynamics including independent component analysis. *J. Neurosci. Methods* 134 (1), 9–21. <https://doi.org/10.1016/j.jneumeth.2003.10.009>.
- Delorme, A., Mullen, T., Kothe, C., Akalin Acar, Z., Bigdely-Shamlo, N., Vankov, A., Makeig, S., 2011. EEGLAB, SIFT, NIFT, BCILAB, and ERICA: new tools for advanced EEG processing. *Comput. Intell. Neurosci.* 2011, 1–12. <https://doi.org/10.1155/2011/130714>.
- Drissi-Daoudi, L., Doerig, A., Herzog, M.H., 2019. Feature integration within discrete time windows. *Nat. Commun.* 10 (1), 4901. <https://doi.org/10.1038/s41467-019-12919-7>.
- Drissi-Daoudi, L., Ögmen, H., Herzog, M.H., 2021. Features integrate along a motion trajectory when object integrity is preserved. *J. Vis.* 21 (12), 4. <https://doi.org/10.1167/jov.21.12.4>.
- Ergenoglu, T., Demiralp, T., Bayraktaroglu, Z., Ergen, M., Beydagi, H., Uresin, Y., 2004. Alpha rhythm of the EEG modulates visual detection performance in humans. *Cognit. Brain Res.* 20 (3), 376–383. <https://doi.org/10.1016/j.cogbrainres.2004.03.009>.
- Fakche, C., & Dugué, L. (2022). *Perceptual cycles travel across retinotopic space* [Preprint]. *Neuroscience*. <https://doi.org/10.1101/2022.05.04.490030>.
- Foxe, J.J., Snyder, A.C., 2011. The role of alpha-band brain oscillations as a sensory suppression mechanism during selective attention. *Front. Psychol.* 2 <https://doi.org/10.3389/fpsyg.2011.00154>.
- Friston, K., 2005. A theory of cortical responses. *Philosoph. Trans. R. Soc. B* 360 (1456), 815–836. <https://doi.org/10.1098/rstb.2005.1622>.
- Frömer, R., Maier, M., Abdel Rahman, R., 2018. Group-Level EEG-Processing Pipeline for Flexible Single Trial-Based Analyses Including Linear Mixed Models. *Front. Neurosci.* 12, 48. <https://doi.org/10.3389/fnins.2018.00048>.
- Gallot, S., Sack, A.T., Schuhmann, T., de Graaf, T.A., 2017. Oscillatory correlates of visual consciousness. *Front. Psychol.* 8, 1147. <https://doi.org/10.3389/fpsyg.2017.01147>.
- Grabot, L., Kayser, C., van Wassenhove, V., 2021. Postdiction: when temporal regularity drives space perception through prestimulus alpha oscillations. *eNeuro* 8 (5). <https://doi.org/10.1523/ENEURO.0030-21.2021>.
- Grootswagers, T., Cichy, R.M., Carlson, T.A., 2018. Finding decodable information that can be read out in behaviour. *Neuroimage* 179, 252–262. <https://doi.org/10.1016/j.neuroimage.2018.06.022>.
- Grootswagers, T., Wardle, S.G., Carlson, T.A., 2017. Decoding dynamic brain patterns from evoked responses: a tutorial on multivariate pattern analysis applied to time series neuroimaging data. *J. Cogn. Neurosci.* 29 (4), 677–697. <https://doi.org/10.1162/jocn.a.01068>.
- Hanslmayr, S., Klimesch, W., Sauseng, P., Gruber, W., Doppelmayr, M., Freunberger, R., Pecherstorfer, T., 2005. Visual discrimination performance is related to decreased alpha amplitude but increased phase locking. *Neurosci. Lett.* 375 (1), 64–68. <https://doi.org/10.1016/j.neulet.2004.10.092>.
- Haufe, S., Meinecke, F., Görgen, K., Dähne, S., Haynes, J.-D., Blankertz, B., Bießmann, F., 2014. On the interpretation of weight vectors of linear models in multivariate neuroimaging. *Neuroimage* 87, 96–110. <https://doi.org/10.1016/j.neuroimage.2013.10.067>.
- Herzog, M.H., Drissi-Daoudi, L., Doerig, A., 2020. All in good time: long-lasting postdictive effects reveal discrete perception. *Trends Cogn. Sci. (Regul. Ed.)* 24 (10), 826–837. <https://doi.org/10.1016/j.tics.2020.07.001>.
- Herzog, M.H., Kammer, T., Scharnowski, F., 2016. Time slices: what is the duration of a percept? *PLoS Biol.* 14 (4), e1002433 <https://doi.org/10.1371/journal.pbio.1002433>.
- Hesselmann, G., Kell, C.A., Eger, E., Kleinschmidt, A., 2008a. Spontaneous local variations in ongoing neural activity bias perceptual decisions. *Proc. Natl. Acad. Sci.* 105 (31), 10984–10989. <https://doi.org/10.1073/pnas.0712043105>.
- Hesselmann, G., Kell, C.A., Kleinschmidt, A., 2008b. Ongoing activity fluctuations in HMT+ bias the perception of coherent visual motion. *Journal of Neurosci.* 28 (53), 14481–14485. <https://doi.org/10.1523/JNEUROSCI.4398-08.2008>.
- Himmelstoss, N.A., Brötzner, C.P., Zauner, A., Kerschbaum, H.H., Gruber, W., Lechinger, J., Klimesch, W., 2015. Prestimulus amplitudes modulate P1 latencies and evoked traveling alpha waves. *Front. Hum. Neurosci.* 9 <https://doi.org/10.3389/fnhum.2015.00302>.
- Hyvärinen, A., Oja, E., 2000. Independent component analysis: algorithms and applications. *Neural Netw.* 13 (4–5), 411–430. [https://doi.org/10.1016/S0893-6080\(00\)00026-5](https://doi.org/10.1016/S0893-6080(00)00026-5).
- Iemi, L., Gwilliams, L., Samaha, J., Aukstulewicz, R., Cycowicz, Y.M., King, J.-R., Nikulin, V.V., Thesen, T., Doyle, W., Devinsky, O., Schroeder, C.E., Melloni, L., Haegens, S., 2022. Ongoing neural oscillations influence behavior and sensory representations by suppressing neuronal excitability. *Neuroimage* 247, 118746. <https://doi.org/10.1016/j.neuroimage.2021.118746>.
- Jensen, O., Mazaheri, A., 2010. Shaping functional architecture by oscillatory alpha activity: gating by inhibition. *Front. Hum. Neurosci.* 4, 186.
- Jensen, O., Pan, Y., Frisson, S., Wang, L., 2021. An oscillatory pipelining mechanism supporting previewing during visual exploration and reading. *Trends Cogn. Sci. (Regul. Ed.)* 25 (12), 1033–1044. <https://doi.org/10.1016/j.tics.2021.08.008>.
- Kayser, S.J., McNair, S.W., Kayser, C., 2016. Prestimulus influences on auditory perception from sensory representations and decision processes. *Proc. Natl. Acad. Sci.* 113 (17), 4842–4847. <https://doi.org/10.1073/pnas.1524087113>.
- Keitel, C., Ruzzoli, M., Dugué, L., Busch, N.A., Benwell, C.S.Y., 2022. Rhythms in cognition: the evidence revisited. *Eur. J. Neurosci.* 55 (11–12), 2991–3009. <https://doi.org/10.1111/ejn.15740>.
- Kelly, S.P., Lalor, E.C., Reilly, R.B., Foxe, J.J., 2006. Increases in alpha oscillatory power reflect an active retinotopic mechanism for distracter suppression during sustained visuospatial attention. *J. Neurophysiol.* 95 (6), 3844–3851. <https://doi.org/10.1152/jn.01234.2005>.
- Kienitz, R., Schmid, M.C., Dugué, L., 2022. Rhythmic sampling revisited: experimental paradigms and neural mechanisms. *Eur. J. Neurosci.* 55 (11–12), 3010–3024. <https://doi.org/10.1111/ejn.15489>.
- Klimesch, W., 2012. Alpha-band oscillations, attention, and controlled access to stored information. *Trends Cogn. Sci. (Regul. Ed.)* 16 (12), 606–617.
- Klimesch, W., 2018. The frequency architecture of brain and brain body oscillations: an analysis. *Eur. J. Neurosci.* 48 (7), 2431–2453. <https://doi.org/10.1111/ejn.14192>.
- Kok, P., Jehee, J.F.M., de Lange, F.P., 2012. Less is more: expectation sharpens representations in the primary visual cortex. *Neuron* 75 (2), 265–270. <https://doi.org/10.1016/j.neuron.2012.04.034>.
- Kok, P., Mostert, P., De Lange, F.P., 2017. Prior expectations induce prestimulus sensory templates. *Proc. Natl. Acad. Sci.* 114 (39), 10473–10478. <https://doi.org/10.1073/pnas.1705652114>.
- Kononowicz, T.W., van Wassenhove, V., 2016. In search of oscillatory traces of the internal clock. *Front. Psychol.* 7 <https://doi.org/10.3389/fpsyg.2016.00224>.
- Latour, P.L., 1967. Evidence of internal clocks in the human operator. *Acta Psychol. (Amst)* 27, 341–348. [https://doi.org/10.1016/0001-6918\(67\)90078-9](https://doi.org/10.1016/0001-6918(67)90078-9).
- Ledoit, O., Wolf, M., 2004. A well-conditioned estimator for large-dimensional covariance matrices. *J. Multivar. Anal.* 88 (2), 365–411. [https://doi.org/10.1016/S0047-259X\(03\)00096-4](https://doi.org/10.1016/S0047-259X(03)00096-4).
- Leonardelli, E., Braun, C., Weisz, N., Lithari, C., Occelli, V., Zampini, M., 2015. Prestimulus oscillatory alpha power and connectivity patterns predispose perceptual integration of an audio and a tactile stimulus: prestimulus and Audiotactile Interactions. *Hum. Brain Mapp.* 36 (9), 3486–3498. <https://doi.org/10.1002/hbm.22857>.
- Leske, S., Dalal, S.S., 2019. Reducing power line noise in EEG and MEG data via spectrum interpolation. *Neuroimage* 189, 763–776. <https://doi.org/10.1016/j.neuroimage.2019.01.026>.
- Limbach, K., Corballis, P.M., 2016. Prestimulus alpha power influences response criterion in a detection task: prestimulus alpha power influences response. *Psychophysiology* 53 (8), 1154–1164. <https://doi.org/10.1111/psyp.12666>.
- London, R.E., Benwell, C.S.Y., Cecere, R., Quak, M., Thut, G., Talsma, D., 2022. EEG alpha power predicts the temporal sensitivity of multisensory perception. *Eur. J. Neurosci.* 55 (11–12), 3241–3255. <https://doi.org/10.1111/ejn.15719>.

- Lundqvist, M., Wutz, A., 2022. New methods for oscillation analyses push new theories of discrete cognition. *Psychophysiology* (5), 59. <https://doi.org/10.1111/psyp.13827>.
- Maris, E., Oostenveld, R., 2007. Nonparametric statistical testing of EEG- and MEG-data. *J. Neurosci. Methods* 164 (1), 177–190. <https://doi.org/10.1016/j.jneumeth.2007.03.024>.
- Mathewson, K.E., Gratton, G., Fabiani, M., Beck, D.M., Ro, T., 2009. To see or not to see: prestimulus phase predicts visual awareness. *J. Neurosci.* 29 (9), 2725–2732. <https://doi.org/10.1523/JNEUROSCI.3963-08.2009>.
- Mathewson, K.E., Lleras, A., Beck, D., Fabiani, M., Ro, T., Gratton, G., 2011. Pulsed out of awareness: EEG alpha oscillations represent a pulsed-inhibition of ongoing cortical processing. *Front. Psychol.* 2, 99. <https://doi.org/10.3389/fpsyg.2011.00099>.
- Menétray, M.Q., Vogelsang, L., Herzog, M.H., 2022. A guideline for linking brain wave findings to the various aspects of discrete perception. *Eur. J. Neurosci.* 55 (11–12), 3528–3537. <https://doi.org/10.1111/ejn.15349>.
- Michail, G., Toran Jenner, L., Keil, J., 2022. Prestimulus alpha power but not phase influences visual discrimination of long-duration visual stimuli. *Eur. J. Neurosci.* 55 (11–12), 3141–3153. <https://doi.org/10.1111/ejn.15169>.
- Michalareas, G., Vezoli, J., van Pelt, S., Schoffelen, J.-M., Kennedy, H., Fries, P., 2016. Alpha-Beta and Gamma Rhythms Subserve Feedback and Feedforward Influences among Human Visual Cortical Areas. *Neuron* 89 (2), 384–397. <https://doi.org/10.1016/j.neuron.2015.12.018>.
- Nichols, T.E., Holmes, A.P., 2002. Nonparametric permutation tests for functional neuroimaging: a primer with examples. *Hum. Brain Mapp.* 15 (1), 1–25. <https://doi.org/10.1002/hbm.1058>.
- Otto, T.U., Ögmen, H., Herzog, M.H., 2006. The flight path of the phoenix - the visible trace of invisible elements in human vision. *J. Vis.* 6 (10), 1079–1086. <https://doi.org/10.1167/6.10.7>.
- Otto, T.U., Ögmen, H., Herzog, M.H., 2009. Feature integration across space, time, and orientation. *J. Exp. Psychol. Hum. Percept. Perform.* 35 (6), 1670–1686. <https://doi.org/10.1037/a0015798>.
- Otto, T.U., Ögmen, H., Herzog, M.H., 2010. Attention and non-retinotopic feature integration. *J. Vis.* 10 (12), 8. <https://doi.org/10.1167/10.12.8>.
- Pagnotta, M.F., Pascucci, D., Plomp, G., 2020. Nested oscillations and brain connectivity during sequential stages of feature-based attention. *Neuroimage* 223, 117354. <https://doi.org/10.1016/j.neuroimage.2020.117354>.
- Pagnotta, M.F., Pascucci, D., Plomp, G., 2022. Selective attention involves a feature-specific sequential release from inhibitory gating. *Neuroimage* 246, 118782. <https://doi.org/10.1016/j.neuroimage.2021.118782>.
- Pan, Y., Popov, T., Frisson, S., Jensen, O., 2022. Saccades are locked to the phase of alpha oscillations during natural reading [Preprint]. *Physiology*. <https://doi.org/10.1101/2022.04.10.487681>.
- Park, H., Kayser, C., 2019. Shared neural underpinnings of multisensory integration and trial-by-trial perceptual recalibration in humans. *eLife* 8, e47001. <https://doi.org/10.7554/eLife.47001>.
- Pascucci, D., Hervais-Adelman, A., Plomp, G., 2018. Gating by induced A-Γ asynchrony in selective attention. *Hum. Brain Mapp.* 39 (10), 3854–3870. <https://doi.org/10.1002/hbm.24216>.
- Pascucci, D., Rubega, M., Plomp, G., 2020. Modeling time-varying brain networks with a self-tuning optimized Kalman filter. *PLoS Comput. Biol.* 16 (8), e1007566. <https://doi.org/10.1371/journal.pcbi.1007566>.
- Peylo, C., Hilla, Y., Sauseng, P., 2021. Cause or consequence? Alpha oscillations in visuospatial attention. *Trends Neurosci.* 44 (9), 705–713. <https://doi.org/10.1016/j.tins.2021.05.004>.
- Plomp, G., Mercier, M.R., Otto, T.U., Blanke, O., Herzog, M.H., 2009. Non-retinotopic feature integration decreases response-locked brain activity as revealed by electrical neuroimaging. *Neuroimage* 48 (2), 405–414. <https://doi.org/10.1016/j.neuroimage.2009.06.031>.
- Popov, T., Miller, G.A., Rockstroh, B., Jensen, O., Langer, N., 2021. Alpha oscillations link action to cognition: an oculomotor account of the brain's dominant rhythm [Preprint]. *Neuroscience*. <https://doi.org/10.1101/2021.09.24.461634>.
- Quigley, C., 2022. Forgotten rhythms? Revisiting the first evidence for rhythms in cognition. *Eur. J. Neurosci.* 55 (11–12), 3266–3276. <https://doi.org/10.1111/ejn.15450>.
- Ronconi, L., Oosterhof, N.N., Bonmassar, C., Melcher, D., 2017. Multiple oscillatory rhythms determine the temporal organization of perception. *Proc. Natl Acad. Sci.* 114 (51), 13435–13440. <https://doi.org/10.1073/pnas.1714522114>.
- Ruzzoli, M., Torralba, M., Morís Fernández, L., Soto-Faraco, S., 2019. The relevance of alpha phase in human perception. *Cortex* 120, 249–268. <https://doi.org/10.1016/j.cortex.2019.05.012>.
- Samaha, J., Cohen, M.X., 2022. Power spectrum slope confounds estimation of instantaneous oscillatory frequency. *Neuroimage* 250, 118929. <https://doi.org/10.1016/j.neuroimage.2022.118929>.
- Samaha, J., Iemi, L., Postle, B.R., 2017. Prestimulus alpha-band power biases visual discrimination confidence, but not accuracy. *Conscious. Cogn.* 54, 47–55. <https://doi.org/10.1016/j.concog.2017.02.005>.
- Samaha, J., Postle, B.R., 2015. The Speed of Alpha-Band Oscillations Predicts the Temporal Resolution of Visual Perception. *Curr. Biol.* 25 (22), 2985–2990. <https://doi.org/10.1016/j.cub.2015.10.007>.
- Samaha, J., Sprague, T.C., Postle, B.R., 2016. Decoding and Reconstructing the Focus of Spatial Attention from the Topography of Alpha-band Oscillations. *J. Cogn. Neurosci.* 28 (8), 1090–1097. https://doi.org/10.1162/jocn_a.00955.
- Sanders, L.L.O., Aukstulewicz, R., Hohlefeld, F.U., Busch, N.A., Sterzer, P., 2014. The influence of spontaneous brain oscillations on apparent motion perception. *Neuroimage* 102, 241–248. <https://doi.org/10.1016/j.neuroimage.2014.07.065>.
- Sauseng, P., Klimesch, W., Stadler, W., Schabus, M., Doppelmayr, M., Hanslmayr, S., Gruber, W.R., Birbaumer, N., 2005. A shift of visual spatial attention is selectively associated with human EEG alpha activity. *Eur. J. Neurosci.* 22 (11), 2917–2926. <https://doi.org/10.1111/j.1460-9568.2005.04482.x>.
- Sergent, C., 2018. The offline stream of conscious representations. *Philosoph. Trans. R. Soc. B* 373 (1755), 20170349. <https://doi.org/10.1098/rstb.2017.0349>.
- Sharp, P., Gutteling, T., Melcher, D., Hickey, C., 2022. Spatial attention tunes temporal processing in early visual cortex by speeding and slowing alpha oscillations. *J. Neurosci.* <https://doi.org/10.1523/JNEUROSCI.0509-22.2022>.
- Steen, J., Loeyts, T., Moerkerke, B., Vansteelandt, S., 2017. medflex: an R package for flexible mediation analysis using natural effect models. *J. Stat. Softw.* (11), 76. <https://doi.org/10.18637/jss.v076.i11>.
- Storey, J.D., 2002. A direct approach to false discovery rates. *J. R. Statist. Soc.* 64 (3), 479–498. <https://doi.org/10.1111/1467-9868.00346>.
- Subasi, A., Gursoy, M.I., 2010. EEG signal classification using PCA, ICA, LDA and support vector machines. *Expert Syst. Appl.* 37 (12), 8659–8666. <https://doi.org/10.1016/j.eswa.2010.06.065>.
- Tallon-Baudry, C., 1999. Oscillatory gamma activity in humans and its role in object representation. *Trends Cogn. Sci. (Regul. Ed.)* 3 (4), 151–162. [https://doi.org/10.1016/S1364-6613\(99\)01299-1](https://doi.org/10.1016/S1364-6613(99)01299-1).
- Tallon-Baudry, C., Bertrand, O., Delpuech, C., Pernier, J., 1996. Stimulus specificity of phase-locked and non-phase-locked 40Hz visual responses in human. *J. Neurosci.* 16 (13), 4240–4249. <https://doi.org/10.1523/JNEUROSCI.16-13-04240.1996>.
- Thut, G., 2006. Band electroencephalographic activity over occipital cortex indexes visuospatial attention bias and predicts visual target detection. *J. Neurosci.* 26 (37), 9494–9502. <https://doi.org/10.1523/JNEUROSCI.0875-06.2006>.
- Van Diepen, R.M., Foxe, J.J., Mazaheri, A., 2019. The functional role of alpha-band activity in attentional processing: the current zeitgeist and future outlook. *Curr Opin Psychol* 29, 229–238. <https://doi.org/10.1016/j.copsyc.2019.03.015>.
- van Dijk, H., Schoffelen, J.-M., Oostenveld, R., Jensen, O., 2008. Prestimulus oscillatory activity in the alpha band predicts visual discrimination ability. *J. Neurosci.* 28 (8), 1816–1823. <https://doi.org/10.1523/JNEUROSCI.1853-07.2008>.
- VanRullen, R., 2016a. How to evaluate phase differences between trial groups in ongoing electrophysiological signals. *Front. Neurosci.* 10 <https://doi.org/10.3389/fnins.2016.00426>.
- VanRullen, R., 2016b. Perceptual cycles. *Trends Cogn. Sci. (Regul. Ed.)* 20 (10), 723–735. <https://doi.org/10.1016/j.tics.2016.07.006>.
- VanRullen, R., Dubois, J., 2011. The psychophysics of brain rhythms. *Front. Psychol.* 2 <https://doi.org/10.3389/fpsyg.2011.00203>.
- Varela, F.J., Toro, A., Roy John, E., Schwartz, E.L., 1981. Perceptual framing and cortical alpha rhythm. *Neuropsychologia* 19 (5), 675–686. [https://doi.org/10.1016/0028-3932\(81\)90005-1](https://doi.org/10.1016/0028-3932(81)90005-1).
- Wutz, A., Weisz, N., Braun, C., Melcher, D., 2014. Temporal windows in visual processing: 'prestimulus brain state' and 'poststimulus phase reset' segregate visual transients on different temporal scales. *J. Neurosci.* 34 (4), 1554–1565. <https://doi.org/10.1523/JNEUROSCI.3187-13.2014>.
- Zazio, A., Ruhnau, P., Weisz, N., Wutz, A., 2022. Pre-stimulus alpha-band power and phase fluctuations originate from different neural sources and exert distinct impact on stimulus-evoked responses. *Eur. J. Neurosci.* 55 (11–12), 3178–3190. <https://doi.org/10.1111/ejn.15138>.
- Zhou, Y.J., Iemi, L., Schoffelen, J.-M., de Lange, F.P., Haegens, S., 2021. Alpha oscillations shape sensory representation and perceptual sensitivity. *J. Neurosci.* 41 (46), 9581–9592. <https://doi.org/10.1523/JNEUROSCI.1114-21.2021>.